

Electrical and optical bistability in $\text{In}_x\text{Ga}_{1-x}\text{As}$ -GaAs piezoelectric quantum wells

L. R. Wilson, D. J. Mowbray, M. S. Skolnick, V. N. Astratov,* and D. W. Peggs
Department of Physics, University of Sheffield, Sheffield S3 7RH, United Kingdom

G. J. Rees, J. P. R. David, R. Grey, G. Hill, and M. A. Pate
Department of Electronic and Electrical Engineering, University of Sheffield, Sheffield, S1 4DU, United Kingdom
 (Received 27 January 1997)

Optically induced bistability in the electrical and optical characteristics of a (111)*B* piezoelectric, strained $\text{In}_{0.15}\text{Ga}_{0.85}\text{As}$ -GaAs single-quantum-well *p-i-n* structure is reported. We demonstrate that the bistability results from photoinduced electron charge buildup in the quantum well. Charge buildup is enhanced relative to a (100) structure as a consequence of the modified band profile due to the large internal piezoelectric field. A region of hysteresis is observed in the current-voltage characteristics under illumination, with the device being stable in either low- or high-current states. Photoluminescence line-shape analysis and magneto-photoluminescence studies demonstrate that the low- and high-current states correspond to either high or near-zero electron charge (n_s) in the well, respectively. Simulations of the band profiles using the deduced values of n_s are consistent with the existence of the two different current and charge accumulation states. [S0163-1829(97)02627-1]

We report the observation of both electrical and optical bistability in a strained layer, piezoelectric single-quantum-well structure embedded in the intrinsic region of a *p-i-n* diode. We show that the intrinsic bistability corresponds to two stable states of the quantum well (QW), one with large photogenerated electron accumulation in the QW and one with near-zero accumulation. Such electron charge buildup is strongly enhanced in the present strained (111)*B* structures compared to conventional (100) structures. The strain in the (111)*B* case leads to the formation of a large internal piezoelectric (PZ) field (~ 170 kV/cm) in the QW.¹ The direction of the PZ field opposes that of the built-in *p-i-n* field, leading to a sawtooth-shaped band profile. The modified band profile results in enhanced electron capture, enhanced n_s in the QW, and hence the occurrence of the bistable phenomena. Hysteresis is observed in the current-voltage (*I-V*) characteristics under illumination, with photoluminescence (PL) and magneto-PL measurements clearly demonstrating electron accumulation in the single quantum well (SQW) when the sample is in the low-current state.

The bistable phenomena we observe have similar origin to those discussed by Zrenner *et al.* for a GaAs QW, AlAs single barrier structure.² However, the high quality of our sample and, in addition, magnetic-field measurements allow the accurate determination of both the density and sign of the carriers involved in the bistable process. Bistable phenomena have also been reported in a number of other semiconductor devices. These include double-barrier resonant tunneling structures where the bistability arises from charge accumulation in the QW on resonance^{3,4} and self-electro-optic devices where the bistability occurs as a result of the change in electric-field-induced shift of the QW absorption edge under optical illumination.⁵

The sample studied was fabricated by molecular-beam epitaxy (MBE) and grown on an n^+ (111)*B* GaAs substrate misoriented 2° toward the (211) axis. In order of growth the layers consist of $1 \mu\text{m}$ of n^+ GaAs, a $0.610\text{-}\mu\text{m}$ GaAs in-

trinsic region in which the $100\text{-}\text{\AA}$ $\text{In}_{0.15}\text{Ga}_{0.85}\text{As}$ SQW is incorporated centrally, and $0.3 \mu\text{m}$ of p^+ GaAs. Mesa photodiodes $400 \mu\text{m}$ in diameter were fabricated, allowing optical access through an annular contact on the p^+ region. Further details of the growth can be found in Ref. 6. A MBE (100) control sample grown under very similar conditions was also investigated.

Low-temperature *I-V* characteristics, both with and without optical excitation from a Ti:sapphire laser at 1.59 eV , are shown in Fig. 1. With no illumination the sample exhibits

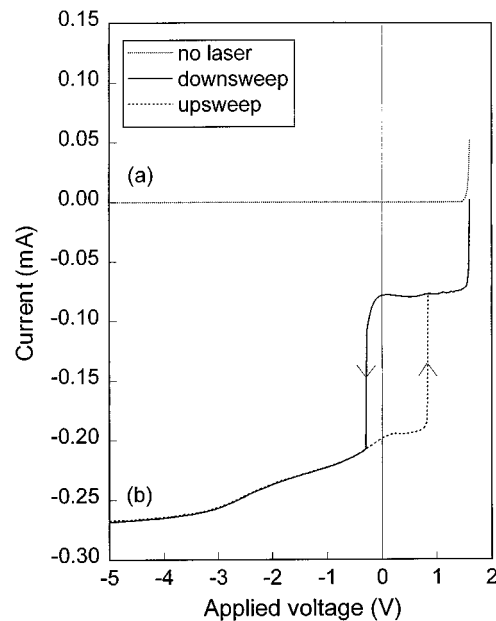


FIG. 1. Low-temperature current-voltage characteristics (a) without optical excitation and (b) with optical excitation at 1.59 eV from a Ti:sapphire laser, with a power density of 4 W/cm^2 . The arrows in (b) indicate the direction of the voltage sweep.

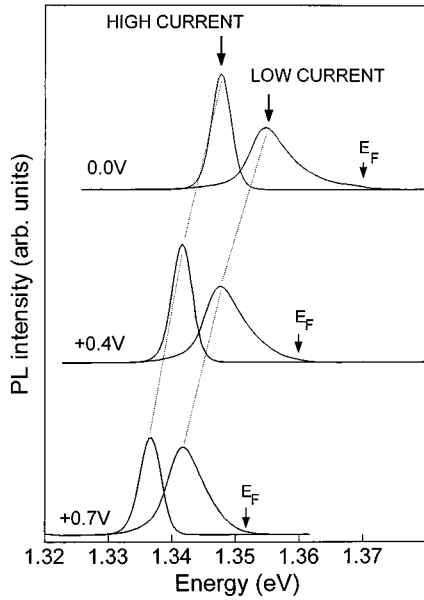


FIG. 2. Photoluminescence spectra at 4.2 K for various bistable voltages. In the low-current state a broad PL band, arising from the recombination of electrons in states from $E=0$ up to E_F , is observed. In the high-current state a much narrower PL band is observed as a result of the near-zero electron density in the well in this state.

typical diodelike characteristics with a small reverse bias leakage current and a reverse breakdown voltage of ~ -20 V, as shown in Fig. 1(a). However, under illumination with light of energy greater than the GaAs band gap (1.52 eV), a region of hysteresis is observed in the I - V characteristics. For applied voltages in this region there are two possible, stable current states: a low-current state on the voltage downsweep branch and a high-current state on the voltage upsweep branch. For any voltage within this hysteresis region a transition from the low-current to the high-current state may be induced by a brief interruption of the optical excitation. As the excitation power density is decreased, the range of voltages over which the hysteresis is observed decreases, eventually collapsing to a step feature for power densities less than 0.1 W/cm². No hysteresis is observed if the laser excites electrons and holes directly into the $\text{In}_x\text{Ga}_{1-x}\text{As}$ SQW (1.30 eV $< h\nu_{\text{laser}} < 1.51$ eV), indicating that the bistability requires the photocreation of carriers in the GaAs barriers and subsequent capture by the SQW. The above bistable phenomena were not observed in the (100) grown control sample.

PL spectra recorded for voltages in the hysteresis region enable the physical mechanisms leading to the bistability to be understood. Figure 2 shows PL spectra taken at various bistable voltages, with the sample in both the low- and high-current state for each voltage. The PL spectra with the sample in the high-current state have a typical linewidth of 5 meV, probably arising from alloy and well width fluctuations. In contrast, PL spectra with the sample in the low-current state are considerably broader with a tail to higher energy, indicative of carrier accumulation in the QW.⁷ In a perfect QW containing a large number of electrons (holes) but relatively few photoexcited holes (electrons), only verti-

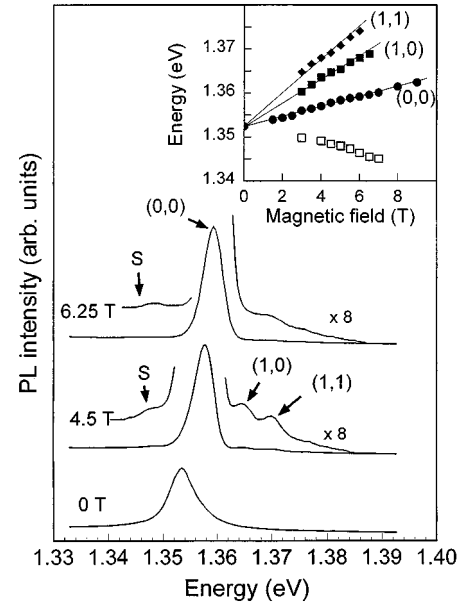


FIG. 3. Magneto-PL spectra measured at 1.8 K with the device at 0.4 V in the low-current state. The peaks labeled (0,0), (1,0), and (1,1) observed at finite magnetic fields arise from the recombination between the electron and hole Landau levels of index (N_e, N_h) . The inset shows the variation of the peak position with the magnetic field. The (N_e, N_h) peaks blueshift with increasing magnetic field. The low-energy peak S is due to shakeup processes and redshifts with increasing magnetic field.

cal transitions close to $k=0$ are allowed. However, the presence of disorder, (e.g., alloy or well width fluctuations) partially lifts the vertical transition selection rule and recombination from all electron states up to the Fermi energy E_F may be observed. In the present sample this gives rise to the weak, high-energy tail in the PL spectra. The relative weakness of this high-energy tail is characteristic of a QW with a low degree of disorder.⁷⁻⁹ The position of the Fermi-edge cutoff E_F is marked on the low-current spectra. The energy difference between the PL peak and E_F provides an estimate for the Fermi energy, which is found to increase from 8.0 meV at an applied voltage of +0.7 V to 13.8 meV at 0 V.

While the above measurements provide evidence for charge buildup in the QW, the sign of the charge carriers is not determined. Magneto-PL measurements confirm the presence of charge accumulation, provide accurate values for n_s , and, in addition, by comparison with the linewidth results, demonstrate that the observed behavior is due to electron accumulation in the QW. Typical magneto-PL spectra, with the device at 0.4 V in the low-current state, are shown in Fig. 3. With an applied magnetic field of 4.5 T, the single, broad zero-field PL line is split into a series of Landau-level (LL) transitions, labeled (N_e, N_h) , which arise from the recombination of electrons and holes from occupied LL's of indices N_e and N_h , respectively.⁷⁻⁹ Recombination between the ground-state electron and hole LL's (0,0) gives rise to the dominant transition in the magneto-PL spectrum with a nominally forbidden, non-Landau-number-conserving transition (1,0) observed to higher energy due to the effects of disorder. The (1,1) transition arises because of a small pho-

to-created hole population in the $N_h = 1$ level.

The inset to Fig. 3 shows a plot of PL peak positions as a function of magnetic field. The energy separation between the two lowest-energy LL transitions corresponds to a cyclotron energy $\hbar\omega_c = \hbar eB/m^*$, where $m^* = 0.07m_0$. This value for the effective mass corresponds to the expected electron effective mass m_{el}^* for $\text{In}_{0.15}\text{Ga}_{0.85}\text{As}$.^{9,10} The separation between the second and third LL transitions is approximately half that between (0,0) and (1,0) and is consistent with that expected for the heavy-hole cyclotron energy (the in-plane heavy hole $m_h^* \approx 0.15m_0$).¹⁰ These results confirm our identification of the LL transitions. The (1,0) and (1,1) transitions are not observed for magnetic fields greater than 6.5 T due to the depopulation of the $N_e = 1$ LL at this field. Using the LL degeneracy $2eB/h$, this gives a value for the density of the charge that builds up in the QW at 0.4 V of $n_s = (3.1 \pm 0.2) \times 10^{11} \text{ cm}^{-2}$. The Fermi energy deduced from the PL linewidth at 0.4 V was 11 meV, corresponding to $n_s = 3.2 \times 10^{11} \text{ cm}^{-2}$, employing the electron mass $m_{el}^* = 0.07m_0$ in the relation $E_F = \hbar^2 \pi n_s / m^*$. This value for n_s is in good agreement with the value of $3.1 \times 10^{11} \text{ cm}^{-2}$ obtained from the magneto-PL, thus confirming that the predominant charge buildup is due to electrons. If instead predominant hole accumulation is assumed and the hole mass of $m_h^* \approx 0.15m_0$ is employed, then $n_s = 1.5 \times 10^{11} \text{ cm}^{-2}$ is obtained from the PL linewidth, in disagreement with the magneto-PL result.

In addition to the main LL transitions, a weak peak, labeled S , is observed to lower energy than (0,0). Its energy separation from (0,0) increases with increasing magnetic field at a rate $\sim 1.3\hbar\omega_c^{el}$. We attribute the low-energy satellite to magnetoplasmon shakeup excitations of the Fermi sea,¹¹ in which an additional electron is promoted to the $N = 1$ LL during the $N = 0$ electron, $N = 0$ hole recombination process. The separation of $\sim 1.3\hbar\omega_c^{el}$ between (0,0) and S is close to that found previously for such magnetoplasmon excitations.¹¹ With the sample in the high-current state the PL shows no splitting and exhibits a diamagnetic shift with increasing magnetic field, consistent with excitonic behavior and indicating negligible carrier accumulation in this state.⁷

The PL and magneto-PL measurements clearly demonstrate that the two current states involved in the bistability are associated with very different electron densities in the QW. Using the values for the electron densities obtained from our measurements we can then model self-consistently the band profiles of the structure corresponding to the two states. Figure 4(a) shows the band profile of the structure at 0 V with no charge in the QW, corresponding to the high-current state. Figure 4(b) shows the calculated, self-consistent band profile at 0 V with the sample in the low-current state and with the experimentally determined QW electron density of $3.9 \times 10^{11} \text{ cm}^{-2}$ deduced from the E_F of 13.8 meV at $V = 0$. The piezoelectric field of $\sim 170 \text{ kV/cm}^6$ gives rise to the large change in slope of the band-edge profiles at the left- and right-hand boundaries of the QW.¹²

As can be seen by inspection of the expanded boxes of Fig. 4, electron capture is expected to be considerably enhanced in the piezoelectric SQW, relative to a conventional (100) grown sample.¹³ This is a consequence of the larger potential barrier to the right-hand side of the SQW, resulting

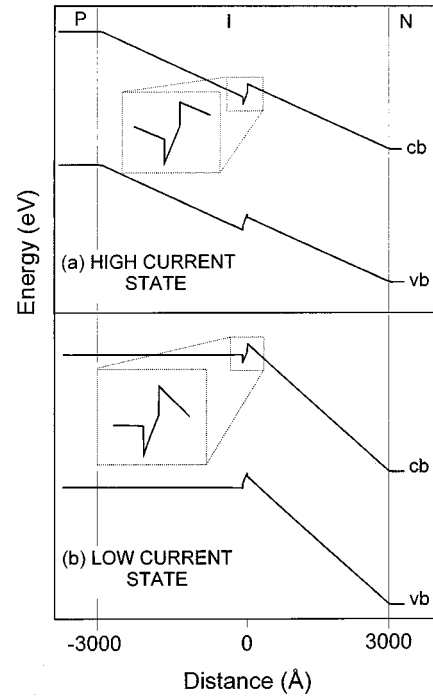


FIG. 4. (a) Calculated band profile of the structure at 0 V with no charge buildup in the QW corresponding to the high-current state. (b) Calculated band profile of the structure at 0 V in the low-current state. The experimentally determined value for the electron density in the SQW of $3.9 \times 10^{11} \text{ cm}^{-2}$ is used in the calculation.

from the internal piezoelectric field, which is in the opposite sense to the built-in p - i - n field. The absorption length of the incident laser light at 1.58 eV is $\sim 1 \mu\text{m}$.¹⁴ Light incident on the sample via the p^+ contact region results in photocreated carrier creation predominantly in the $0.3\text{-}\mu\text{m}$ -thick p^+ contact and in the $0.6\text{-}\mu\text{m}$ i region. Due to the sign of the built-in field (see Fig. 4), electrons (and not holes) created in the p^+ region will be injected into the i region and drift towards the QW. In addition, electrons created in the i region above the QW will also drift towards the QW. In the voltage region from +1.5 V to 0 V, some of these electrons will become trapped in the QW, giving rise to the band profile of Fig. 4(b), which corresponds to the low-current branch of the I - V characteristics. The current is reduced in this state because now only those carriers photocreated in the region to the right of the QW are swept out to the contacts by the remaining electric field. No further electron accumulation occurs beyond the band profile of Fig. 4(b) as the intrinsic region to the left of the QW is almost flat. The small number of electrons that continue to be captured replenish those that are lost from the QW by tunneling or recombination. With increasing reverse bias the electric field in the region to the right of the QW increases, leading to a decrease in the effective width of the potential barrier on the right-hand side of the well. Eventually significant electron tunneling out of the well can occur, the well rapidly empties, and the device switches to the high-current state. When the bias is swept from negative to positive the band profile is of a form similar to that shown in Fig. 4(a), which is less favorable for charge

buildup due to the higher electric field in the barrier, and the device remains in the high-current, low-accumulation state. Our band profile modeling thus demonstrates that two distinct states exist for all applied voltages throughout the region of hysteresis, consistent with the observation of bistability.

In conclusion, we have studied a piezoelectric single-quantum-well *p-i-n* structure that exhibits both electrical and optical bistability under illumination. The large internal piezoelectric field results in a band profile that enhances electron capture by the QW resulting in the observed bista-

bility. Optical measurements provide conclusive evidence for the occurrence of electron accumulation in one of the states and allow the electron density to be determined. Using the experimentally determined electron densities, the band profiles of the structure have been modeled self-consistently and found to be consistent with the occurrence of the bistability.

We wish to acknowledge financial support from the Engineering and Physical Sciences Research Council (EPSRC) Grant No. GR/H45773. D.J.M. acknowledges financial support from EPSRC.

*Permanent address: A. F. Ioffe Physico-Technical Institute, 194021 St. Petersburg, Russia.

¹D. L. Smith, *Solid State Commun.* **57**, 919 (1986).

²A. Zrenner, J. M. Worlock, L. T. Florez, J. P. Harbison, and S. A. Lyon, *Appl. Phys. Lett.* **56**, 18 (1990).

³E. S. Alves, L. Eaves, M. Henini, O. H. Hughes, M. L. Leadbeater, F. W. Sheard, and G. A. Toombs, *Electron. Lett.* **24**, 1190 (1988).

⁴F. W. Sheard and G. A. Toombs, *Appl. Phys. Lett.* **54**, 1228 (1988).

⁵D. A. B. Miller, D. S. Chemla, T. C. Damen, A. C. Gossard, W. Wiegmann, T. H. Wood, and C. A. Burrus, *Appl. Phys. Lett.* **45**, 13 (1984).

⁶J. P. R. David, R. Grey, G. J. Rees, A. S. Pabla, T. E. Sale, J. Woodhead, J. L. Sanchez-Rojas, M. A. Pate, G. Hill, P. N. Robson, R. A. Hogg, T. A. Fisher, M. S. Skolnick, D. M. Whittaker, A. R. K. Willcox, and D. J. Mowbray, *J. Electron. Mater.* **23**, 978 (1994); R. A. Hogg *et al.*, *Phys. Rev. B* **48**, 8491 (1993).

⁷M. S. Skolnick, K. J. Nash, M. K. Saker, S. J. Bass, P. A. Claxton, and J. S. Roberts, *Appl. Phys. Lett.* **50**, 26 (1987).

⁸M. S. Skolnick, D. G. Hayes, P. E. Simmonds, A. W. Higgs, G. W. Smith, H. J. Hutchinson, C. R. Whitehouse, L. Eaves, M. Henini, and D. H. Hughes, *Phys. Rev. B* **41**, 10 754 (1990).

⁹P. E. Simmonds, M. S. Skolnick, T. A. Fisher, K. J. Nash, and R. S. Smith, *Phys. Rev. B* **45**, 9497 (1992).

¹⁰E. D. Jones, S. K. Lye, F. J. Fritze, J. F. Klem, J. E. Schirber, C. P. Tigges, and T. J. Drummond, *Appl. Phys. Lett.* **54**, 2227 (1989).

¹¹K. J. Nash, M. S. Skolnick, M. K. Saker, and S. J. Bass, *Phys. Rev. Lett.* **70**, 3115 (1993).

¹²Calculation of the *E1-HH1* transition energies for the band profiles of Figs. 4(a) and 4(b) leads to the prediction of a blueshift of the transition energies between the $n_s=0$ and $3.4 \times 10^{11} \text{ cm}^{-2}$ states of 7 meV. This value is in good agreement with the observed blueshift of 6 meV of Fig. 2 (0.4-V spectra), providing further confidence in the modelling of the two stable current states. The blueshift arises as a result of the reduction of the electric field in the QW in the low-current, high-charge state.

¹³In the GaAs QW, AlAs barrier sample investigated by Zrenner *et al.* in Ref. 2, charge capture by the QW is enhanced by the presence of the AlAs barrier. These workers attributed the increased PL linewidths they observed to the enhancement of hole accumulation in the QW by the large valence-band barrier at the GaAs-AlAs interface. However, they pointed out that the occurrence of electron accumulation could not be excluded. In fact, the large linewidths they observe of ~ 40 meV may be more consistent with electron charge buildup due to the factor of at least 2 lighter electron mass relative to that for heavy holes.

¹⁴D. E. Aspnes and A. A. Studna, *Phys. Rev. B* **27**, 985 (1983).